November 2006

Quantitative Membrane Loading of Polymer Vesicles

P. Peter Ghoroghchian
University of Pennsylvania

John J. Lin
University of Pennsylvania

Aaron K. Brannon
University of Minnesota

Paul R. Frail
University of Pennsylvania

Frank S. Bates
University of Minnesota

See next page for additional authors

Quantitative Membrane Loading of Polymer Vesicles

Abstract
We utilize a series of structurally homologous, multi-porphyrin-based, fluorophores (PBFs) in order to explore the capacity of polymer vesicles (polymersomes) to stably incorporate large hydrophobic molecules, non-covalently within their thick lamellar membranes. Through aqueous hydration of dry, uniform thin-films of amphiphilic polymer and PBF species deposited on Teflon, self-assembled polymersomes are readily generated incorporating the hydrophobic fluorophores in prescribed molar ratios within their membranes. The size-dependent spectral properties of the PBFs allow for ready optical verification (*via* steady-state absorption and emission spectroscopy) of the extent of vesicle membrane loading and enable delineation of intermembranous molecular interactions. The resultant effects of PBF membrane-loading on polymersome thermodynamic and mechanical stability are further assessed by cryogenic transmission electron microscopy (cryo-TEM) and micropipet aspiration, respectively. We demonstrate that polymersomes can be loaded at up to 10 mol/wt% concentrations, with hydrophobic molecules that possess sizes comparable to those of large pharmaceutical conjugates (*e.g.* ranging 1.4–5.4 nm in length and Mw = 0.7–5.4 kg mol^{-1}), without significantly compromising the robust thermodynamic and mechanical stabilities of these synthetic vesicle assemblies. Due to membrane incorporation, hydrophobic encapsulants are effectively prevented from self-aggregation, able to be highly concentrated in aqueous solution, and successfully shielded from deleterious environmental interactions. Together, these studies present a generalized paradigm for the generation of complex multi-functional materials that combine both hydrophilic and hydrophobic agents, in mesoscopic dimensions, through cooperative self-assembly.

Comments
For personal or professional use only; May not be further made available or distributed. Reprinted from *Soft Matter*, Volume 2, Issue 11, November 7, 2006, pages 973-980.

Author(s)
P. Peter Ghoroghchian, John J. Lin, Aaron K. Brannon, Paul R. Frail, Frank S. Bates, Michael J. Therien, and Daniel A. Hammer

Quantitative membrane loading of polymer vesicles

P. Peter Ghoroghchian,[ab] John J. Lin,[a] Aaron K. Brannan,[c] Paul R. Frail,[b] Frank S. Bates,[c] Michael J. Therien*[b] and Daniel A. Hammer*[a]

Received 27th March 2006, Accepted 11th August 2006
First published as an Advance Article on the web 20th September 2006
DOI: 10.1039/b604212k

We utilize a series of structurally homologous, multi-porphyrin-based, fluorophores (PBFs) in order to explore the capacity of polymer vesicles (polymersomes) to stably incorporate large hydrophobic molecules, non-covalently within their thick lamellar membranes. Through aqueous hydration of dry, uniform thin-films of amphiphilic polymer and PBF species deposited on Teflon, self-assembled polymersomes are readily generated incorporating the hydrophobic fluorophores in prescribed molar ratios within their membranes. The size-dependent spectral properties of the PBFs allow for ready optical verification (*via* steady-state absorption and emission spectroscopy) of the extent of vesicle membrane loading and enable delineation of intermembranous molecular interactions. The resultant effects of PBF membrane-loading on polymersome thermodynamic and mechanical stability are further assessed by cryogenic transmission electron microscopy (cryo-TEM) and micropipet aspiration, respectively. We demonstrate that polymersomes can be loaded at up to 10 mol/wt% concentrations, with hydrophobic molecules that possess sizes comparable to those of large pharmaceutical conjugates (*e.g.* ranging 1.4–5.4 nm in length and Mw = 0.7–5.4 kg mol^{-1}), without significantly compromising the robust thermodynamic and mechanical stabilities of these synthetic vesicle assemblies. Due to membrane incorporation, hydrophobic encapsulants are effectively prevented from self-aggregation, able to be highly concentrated in aqueous solution, and successfully shielded from deleterious environmental interactions. Together, these studies present a generalized paradigm for the generation of complex multi-functional materials that combine both hydrophilic and hydrophobic agents, in mesoscopic dimensions, through cooperative self-assembly.

Introduction

Developments in the emerging field of nanobiotechnology promise to have many important clinical implications. Synthetic soft materials (including polymers, peptides, and lipids) have been designed to self-assemble into complex architectures and serve as useful nanocontainers in aqueous solution.[1–4] For example, liposomes (vesicles comprised of natural phospholipids) have long been utilized to encapsulate aqueous soluble imaging and therapeutic agents in high concentrations.[5] Despite improvements in drug toxicity and pharmacokinetic profiles associated with these encapsulated formulations, several factors have hampered the generalized biomedical adoption of lipid vesicles: these include, 1) chemical and mechanical attributes that render the vehicle unstable, 2) short blood circulation half-lives, and 3) difficulties in achieving high drug/lipid ratios of *hydrophobic* agents without resorting to covalent chemical modification.[5–7]

More recently, polymersomes (50 nm–50 μm diameter synthetic polymer vesicles) have been formed from a number of amphiphiles, offering a rich diversity in chemical and material properties.[8–12] Through synthetic chemistry, rational control of block copolymer compositions is readily achieved and has enabled the generation of polymer vesicles that are substantially more stable than their phospholipid-based counterparts; polymersomes have been further designed to systematically degrade over longer timescales.[13] Dependent upon the molecular weight of their component amphiphiles, polymersomes also possess a membrane core thickness that can vary between 5–50 nm, affording enormous mechanical strength that makes them 5–50 times tougher than liposomes, even when in the fluid state.[14] In expanding the utility of conventional vesicles beyond aqueous encapsulation, we have previously demonstrated that thick polymersome membranes can uniquely incorporate numerous large, hydrophobic, multi-porphyrin (**PZn**)-based near infrared (NIR) fluorophores (NIRFs)[15–18] stably through non-covalent interactions;[19,20] these self-assembled NIR-emissive polymersomes define a soft matter platform that enables optically-based methods[21,22] for deep-tissue imaging.

[a]*School of Engineering and Applied Science, and Institute for Medicine and Engineering, University of Pennsylvania, 120 Hayden Hall, 3320 Smith Walk, Philadelphia, PA 19104-6323, USA. E-mail: hammer@seas.upenn.edu; Fax: +1 215-573-2071; Tel: +1 215-573-6771*
[b]*Department of Chemistry, University of Pennsylvania, 231 South 34th Street, Philadelphia, PA 19104-6323, USA. E-mail: therien@sas.upenn.edu; Fax: +1 215-898-6242; Tel: +1 215-898-0087*
[c]*Department of Chemical Engineering and Materials Science, University of Minnesota, 151 Amundson Hall, 421 Washington Avenue SE, Minneapolis, MN 55455, USA*

Here, we demonstrate the reproducible and quantitative loading of variously sized hydrophobic molecules within synthetic polymersome membranes, systematically evaluating the nano- and microscopic effects on the resultant vesicles' structural and material properties. A 4-hydroxybenzoate-terminated polyethyleneoxide-block-polybutadiene copolymer (PEO_{30}-b-PBD_{46}, Mw = 3800 g mol^{-1}) was utilized in order to yield self-assembled polymersomes with a membrane core thickness of 9.6 nm. In general, there is a paucity of emissive molecules of such large size and comparable molecular dimensions to that of the polymersome membranes. As our emissive models, we chose a series of structurally homologous multi-porphyrin-based fluorophores (PBFs) that are insoluble in aqueous solution (Fig. 1); these mono-, tri-, and penta-PZn structures, (**PZn_1**, **PZn_3**, and **PZn_5**: ranging 1.4–5.4 nm in length and 0.7–5.4 kg mol^{-1} in Mw) possessing a *meso*-to-*meso* ethyne-bridged linkage,[17] have molecular lengths of approximately 1/4, 1/3, and 1/2 of the membrane core thickness, respectively (Fig. 1). Through aqueous hydration of dry, uniform thin-films of amphiphilic polymer and PBF deposited on Teflon, self-assembled polymersomes are readily generated incorporating the hydrophobic fluorophores in prescribed molar ratios within their membranes. The resultant effects of PBF dimensions on intermembranous molecular packing and vesicle mechanical stability are examined as a function of the extent of fluorophore membrane loading. These studies show that polymersome membranes can stably accommodate up to 10 mol% of each of these hydrophobic supermolecular fluorophores (corresponding to 2, 8, and 14 wt% **PZn_1**, **PZn_3**, and **PZn_5**, respectively) without compromising the robust thermodynamic and mechanical stabilities of their synthetic lamellar structures.

Results and discussion

Steady-state absorption spectroscopic and cryo-TEM studies of PBF membrane-incorporation

Small (<300 nm diameter) emissive polymersomes were produced by aqueous rehydration and sonication of thin-film formulations varying in the molar ratios of polymer to PBF (**PZn_1**, **PZn_3**, **PZn_5**) deposited on Teflon. Increasing conjugation length in **PZn_1**–**PZn_5** augments the NIR absorption oscillator strength and shifts both the fluorophore low-energy absorption band and corresponding emission maximum progressively to longer wavelengths.[15–18] As the 4-hydroxybenzoate-terminated polymer ($\lambda_{abs.\ max.}$ = 255 nm) and PBFs **PZn_1** ($\lambda_{abs.\ max.}$ = 428 nm), **PZn_3** ($\lambda_{abs.\ max.}$ = 794 nm) and **PZn_5** ($\lambda_{abs.\ max.}$ = 861 nm) have non-overlapping absorption maxima in aqueous vesicle suspensions, their electronic absorption spectra were monitored independently and the concentrations of polymer and PBF in solution were calculated using Beer's Law. When the molar ratio of polymer : PBF deposited on Teflon exceeded 10 : 1, there was a near perfect correlation with the resultant polymer : PBF molar ratio composing the vesicles' membrane structures (Fig. 2A), as well as a greater than 50% uptake of the mass of Teflon-deposited fluorophore into the membranes of the water-soluble polymersomes (Fig. 2B); note, **PZn_3** and **PZn_5** possess no aqueous solubility in the absence of the vesicles' host membranes. Further, the yield of vesicles based on the total amount of Teflon-deposited polymer ranged from 75–80% for each polymer : PBF formulation (Fig. 2C).

As depicted in Fig. 3, polymersomes have a significant capacity to solvate these large, hydrophobic, supermolecular fluorophores within their thick membranes; cryogenic transmission electron microscope (cryo-TEM) images of aqueous

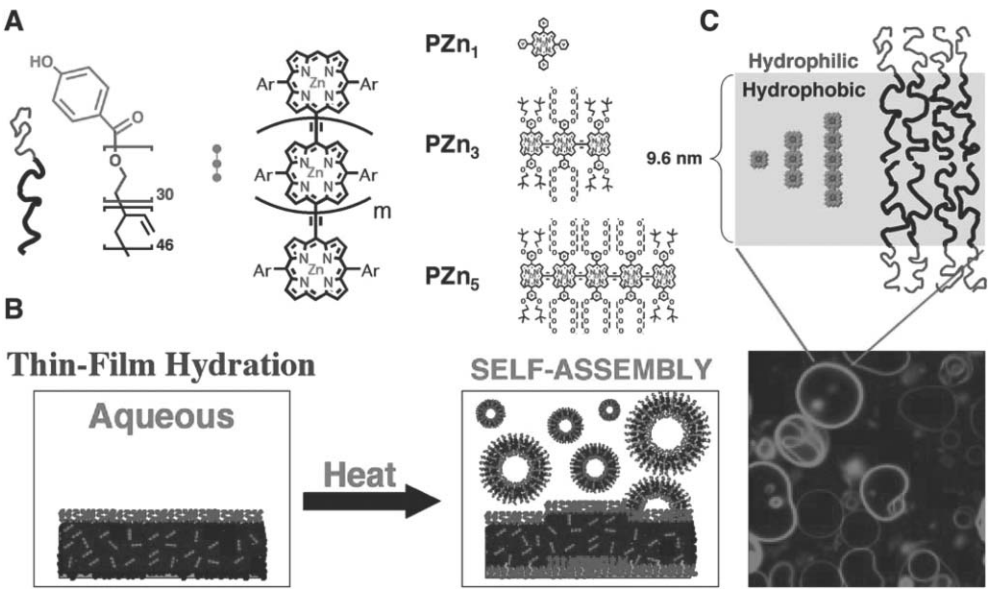

Fig. 1 Membrane loading of polymersomes through cooperative self-assembly. (A) Chemical structures of 4-hydroxy-benzoate-terminated polyethyleneoxide-block-polybutadiene (PEO_{30}-b-PBD_{46}, Mw = 3800 g mol^{-1}) and *meso*-to-*meso* ethynyl-bridged oligo[porphyrin]-based fluorophores (PBFs) **PZn_3**, **PZn_5**, and the **PZn_1** benchmark. (B) Schematic depicting the self-assembly of emissive polymersomes. (C) Relative sizes of PBFs as compared to the thickness of the vesicle membrane and scanning confocal microscope image of giant (>1 μm diameter) emissive polymersomes loaded with **PZn_3** (experimental conditions: T = 23 °C, DI water).

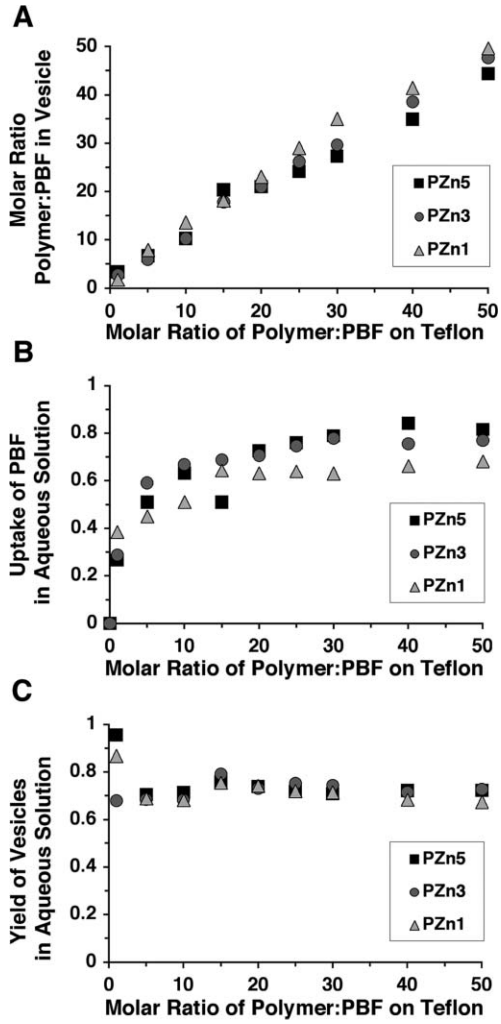

Fig. 2 Polymersomes accommodating hydrophobic oligo[porphyrin]-based fluorophores (PBFs) of various sizes. (A) The polymer : PBF ratio composing the vesicles' membranes, (B) membrane-uptake of PBF into aqueous vesicle suspensions, and (C) the yield of emissive polymersomes in aqueous solution, each as a function of the polymer : PBF molar ratio originally deposited on Teflon, as determined by electronic absorption spectroscopy. Experimental conditions: T = 23 °C, DI water.

suspensions, produced from thin-film formulations deposited at up to 10 : 1 molar ratio of polymer : PBF, demonstrate that even at large membrane loading levels (~10 mol/wt%), the fluorophores do not interfere with self-assembly, nor introduce a thermodynamic driving force that alters the vesicles' bilayer structure in favor of other arrangements such as inverse structures, coalesced vesicles, or even phase separation. Moreover, these aqueous-insoluble fluorophores can be readily dispersed at bulk solution concentrations greater than 1 mM (3–5 mg mL^{-1} in DI water) *via* membrane incorporation within aqueous vesicle suspensions. Further, the membrane-encapsulated formulations are stable at room temperature as measured after several months *via* dynamic light scattering and steady-state absorption spectroscopy (data not shown).

We next examined the absorption spectra of aqueous polymersome solutions formed from thin-film formulations deposited in decreasing molar ratios of polymer : PBF; normalizing these spectra by the calculated concentration of emitters yielded the absorption extinction coefficients (ε, M^{-1} cm^{-1}) for each PBF species dependent upon the extent of membrane-loading per vesicle (Fig. 4). At molar ratios of polymer : PBF which exceeded 10 : 1 (*i.e.* <10 mol% membrane loading levels), there was no significant change in either the calculated ε, the spectral shape, nor peak absorbance wavelength of $\mathbf{PZn_3}$ or $\mathbf{PZn_5}$ dependent upon the degree of vesicle loading; at higher membrane loading levels (>10 mol%), such electronic spectral changes consistent with significant fluorophore–fluorophore aggregation were evident. Notably, for $\mathbf{PZn_1}$, similar alterations in the absorption spectra were present at lower loadings, due likely to differences in membrane packing that derive from $\mathbf{PZn_1}$'s four-fold symmetry and meso-aryl groups lacking solubilizing substituents (Fig. 1).

We have previously demonstrated that SOPC-based liposomes can only incorporate the smaller **PZn**-based fluorophores ($\mathbf{PZn_1}$ and $\mathbf{PZn_2}$) at <1 mol% membrane-loading levels.[19] Consistent with studies that have investigated the liposomal incorporation of hydrophobic porphyrin-based photosensitizers[23–25] or other fluorescent membrane probes,[6] larger liposomal loading levels (>1 mol%) generally result in significant intermembranous molecular aggregation. That no observable quantity of longer-wavelength emitting $\mathbf{PZn_3}$–$\mathbf{PZn_5}$ can be incorporated within SOPC-based liposomes likely stems from the fact that the molecular lengths of these species (3.2–5.4 nm) approach or exceed the thickness of conventional lipid membranes (3–5 nm). In contrast, $\mathbf{PZn_3}$–$\mathbf{PZn_5}$ are of relatively small size when compared to the thickness of the polymersome bilayer membrane (9.6 nm), and lead to little or no alteration in the membrane structure upon their non-covalent incorporation.

Steady-state fluorescence spectroscopic studies

We further sought to correlate changes in the molecular packing of hydrophobic encapsulants with the extent of membrane loading and their relative sizes as compared to the thickness of the polymersome membrane. Aqueous suspensions of small (<300 nm diameter) emissive polymersomes were formed from thin-film formulations deposited at various molar ratios of PEO_{30}-b-PBD_{46}-based copolymer and PBFs $\mathbf{PZn_3}$ and $\mathbf{PZn_5}$. The solutions were then diluted, in order to obtain bulk concentrations of emitters within the linear range of fluorescence detection (*i.e.* less than or equal to 0.05 absorbance units), and their fluorescence spectra were recorded (Fig. 5). By spectral comparison, emissive polymersomes formed from decreasing (ranging from 1000 : 1 to 10:1) molar ratios of polymer : PBF showed marked decreases in their respective fluorescence signal intensities, when normalized by the total number of emitters per vesicle, but a near invariant $\lambda_{em.\ max.}$. These results suggest that the diminished emissive output per PBF with increasing vesicle membrane-loading derives largely from concentration dependent energy-transfer dynamics to dark trap sites, rather than from PBF quenching dominated by loading-dependent fluorophore aggregation.[26] Because $\mathbf{PZn_1}$ possesses a substantially lower oscillator-strength Q-state absorption manifold relative to that of $\mathbf{PZn_3}$ and $\mathbf{PZn_5}$, studies examining emissive output per PBF as a function of

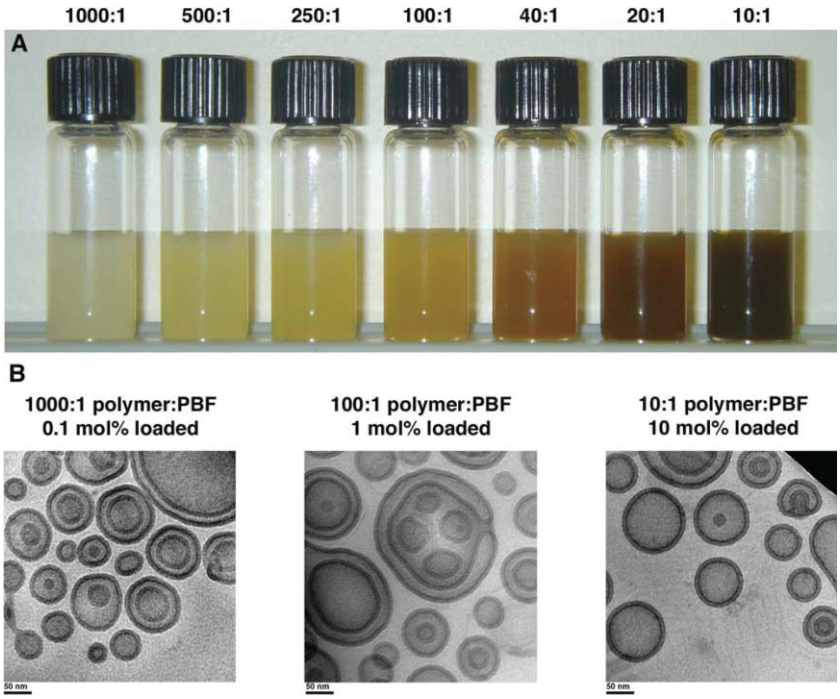

Fig. 3 Capacity of polymersome membranes to stably incorporate and solvate large oligo[porphyrin]-based fluorophores (PBFs). (A) Solution vials containing equal aqueous concentrations of polymer (15 mM) but with increasing amounts of $\mathbf{PZn_3}$, as indicated by the decreasing molar ratios of polymer : PBF (from left to right). (B) Cryo-TEM images of the small (<300 nm diameter) emissive polymersomes formed by aqueous rehydration of various thin-film formulations of polymer and PBF $\mathbf{PZn_3}$. Experimental conditions: T = 23 °C, DI water.

vesicle membrane-loading necessitated B band excitation ($\lambda_{\text{abs. max.}}$ = 428 nm) for $\mathbf{PZn_1}$. Due to the larger contribution of Rayleigh scattering at shorter wavelengths, these data did not allow rigorous comparison of normalized fluorescence emission between various aqueous vesicle suspensions that dispersed the $\mathbf{PZn_1}$ fluorophore.

Upon further quantitative examination, both $\mathbf{PZn_3}$ and $\mathbf{PZn_5}$ displayed a linear decrease in relative fluorescence signal intensity at low mol% membrane loadings (from 0.1–0.4 mol%, corresponding to vesicles formed from 1000 : 1 to 250 : 1 molar ratios of polymer : PBF), but exhibited a mono-exponential decrease upon higher loading (from 1–10 mol%; see Fig. 6A dotted lines). This decrease in the relative emission per molecule was more pronounced in the case of $\mathbf{PZn_5}$ (black) relative to $\mathbf{PZn_3}$ (gray) and indicates that the larger supermolecular fluorophore experiences, as expected, a greater number of intermembranous fluorophore–fluorophore interactions, that lead to energy transfer, at identical membrane concentrations (resulting in an increase in non-radiative decay and loss of fluorescence emission). In order to explore the relative distribution of $\mathbf{PZn_3}$ and $\mathbf{PZn_5}$ within the polymersome membrane, we compared concentration-dependent fluorescence emission of each PBF when loaded within PEO_{30}-b-PBD_{46}-based vesicles (membrane core-thickness d = 9.6 nm; Fig. 6A dotted lines) to that observed in vesicles comprised of the larger PEO_{80}-b-PBD_{125} copolymer (membrane core-thickness d = 14.8 nm; Fig. 6A solid lines).

By increasing membrane thickness, the relative fluorescence emission of $\mathbf{PZn_3}$, at identical fluorophore membrane concentrations, increased, indicating a change in the relative distribution of the $\mathbf{PZn_3}$ fluorophore when incorporated in the thicker PEO_{80}-b-PBD_{125}-based polymersome membrane. In contrast, $\mathbf{PZn_5}$ displayed nearly identical concentration-dependent fluorophore emission intensities within both polymersome environments, consistent with a similar relative fluorophore distribution irrespective of membrane thickness. Compared to $\mathbf{PZn_3}$, the $\mathbf{PZn_5}$ fluorophore possesses a greater number of 9-methoxy-1,4,7-trioxanonyl aryl-substituents that likely influence its localization more predominantly to the vesicle's aqueous/membrane interface. As a result, increasing membrane core thickness in $\mathbf{PZn_5}$-based polymersomes has little effect on varying fluorophore–fluorophore intermolecular distances and hence results in conserved concentration-dependent fluorophore emission. These results highlight the significant effects of PBF-ancillary-aryl-group substituents in influencing not only intramolecular torsion, and the magnitude of PZn-to-PZn conjugative interactions,[20] but also relative fluorophore distribution when incorporated within polymersome membranes; note, a complete study of substituent-driven PBF dispersion in various polymersome systems, differing in both chemical composition and membrane core thickness, is in progress and the results will be published elsewhere. For each formulation, by multiplying the PBF's normalized fluorescence signal intensity by the number of emitters per vesicle, the total integrated steady-state vesicular-emission was obtained as a function of mol% membrane-loading (Fig. 6B). For both $\mathbf{PZn_3}$- and $\mathbf{PZn_5}$-based vesicles, the maximum steady-state emission intensity per vesicle was observed at an approximately 2.5 mol% membrane-loading level in PEO_{80}-b-PBD_{125}-based polymersomes (corresponding to vesicles produced from 40 : 1 molar ratios of polymer : PBF).

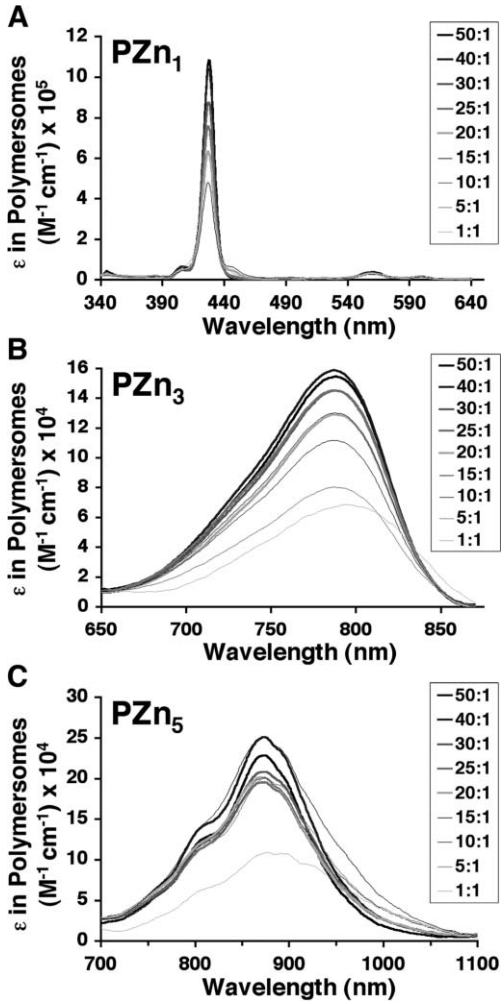

Fig. 4 Absorption extinction coefficients (ε, M^{-1} cm^{-1}) for each oligo[porphyrin]-based fluorophore (PBF) as a function of the polymer : PBF molar ratio composing the vesicles' membranes. Experimental conditions: T = 23 °C, DI water.

Micropipet aspiration of membrane-loaded polymer vesicles

It has previously been demonstrated that polymersomes possess increased mechanical stability as compared to conventional phospholipid vesicles.[9,14] We sought to further examine how the mechanical properties of these synthetic polymer membranes were affected upon PBF incorporation. Several batches of giant (approximately 10 μm diameter) PEO_{30}-b-PBD_{46}-based polymersomes were produced that varied in membrane-loading between 1–10 mol% PBF : polymer. As the bilayer membrane can deform and stretch under tension when the membrane is fluid-like, by utilizing micropipet aspiration[9,14,27,28] the vesicles' mechanical properties were examined. As depicted in Fig. 7A, the vesicles' areal strains (α) were measured, plotted relative to the applied external tensions (τ, mN m^{-1}), and compared to τ *vs.* α for unloaded polymersomes. Incorporation of the large supermolecular fluorophores **PZn_3** and **PZn_5** resulted in only a slight decrease (−18%) in the mechanical toughness of the membrane (area under the stress *vs.* strain curve) and did not significantly alter the critical areal strain

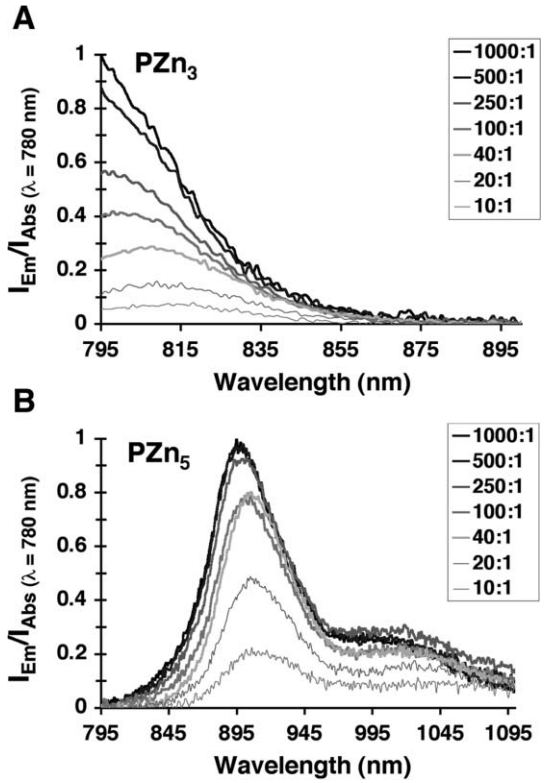

Fig. 5 (A) Fluorescence spectra of PBFs **PZn_3** and **PZn_5** dependent on the molar ratios of polymer : PBF constituting the vesicles' membranes. Spectra were normalized by emitter concentration and plotted on a relative scale of emission intensity.

(the percent of elastic expansion of a vesicle's surface area before rupture).

Compared to liposomes of similar size comprised of SOPC lipids (critical lysis tension = 12 mN m^{-1}; critical areal strain = 6%),[9] membrane-loaded PEO_{30}-b-PBD_{46}-based polymersomes are ~4-fold tougher. While **PZn_3**- and **PZn_5**-based polymer vesicles possessed nearly identical values for the critical lysis tension (22%) and measured mechanical toughness, these values were independent of the extent of fluorophore loading (between 1–10 mol%, corresponding to 0.8–8 wt% **PZn_3** and 1.4–14 wt% **PZn_5**); note, unloaded PEO_{30}-PBD_{46}-based polymersomes possess ~5-fold greater mechanical toughness compared to a benchmark SOPC-based liposome, indicating that extensive PBF loading of the membrane only perturbs vesicle mechanical properties to a minor degree. Additionally, the area elastic moduli (K_a, mN m^{-1}) for **PZn_3**- and **PZn_5**-based polymersomes decreased relative to unloaded vesicles, indicating an increase in membrane compliance, but this decrease did not change upon increased fluorophore loading (Fig. 7B). Furthermore, the calculated bending moduli also did not differ from that of unloaded vesicles (data not shown).

Finally, we compared the membrane core-thickness (d) and average interfacial area per chain (a_o) of polymersomes formed from differing molar ratios of **PZn_3** and the PEO_{30}-b-PBD_{46} copolymer (Table I). It was found that varying membrane loading of this large (approximately 3.2 nm in length; $Mw \approx 3$ kg mol^{-1}) supermolecular fluorophore, between 0.1–10 mol% (0.08–8 wt%), did not perturb the vesicles'

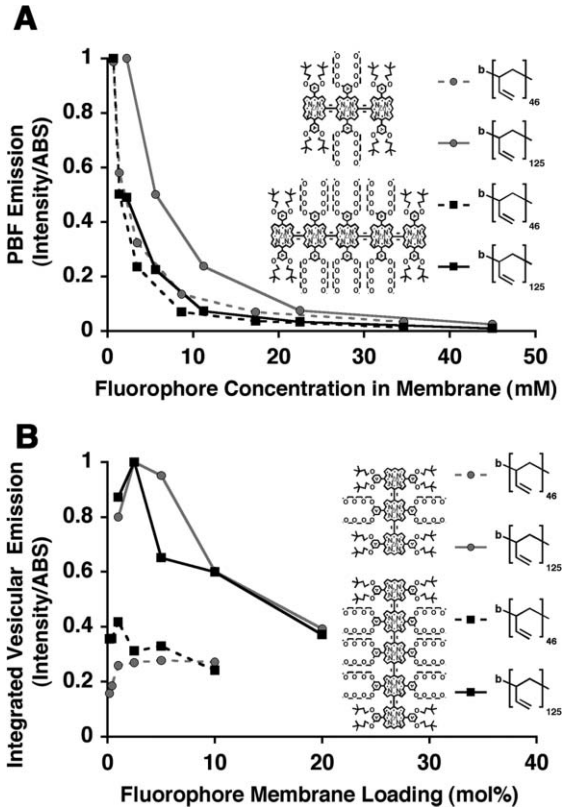

Fig. 6 Comparison of relative emission of oligo[porphyrin]-based fluorophores (PBFs) in aqueous polymersome suspensions as a function of membrane loading (experimental conditions: T = 23 °C, DI water). Quantitative comparison of (A) the fluorescence signal intensity per emitter; and, (B) the total integrated emission per vesicle, as a function of mol% polymersome membrane loading with PBFs **PZn$_3$** and **PZn$_5$**.

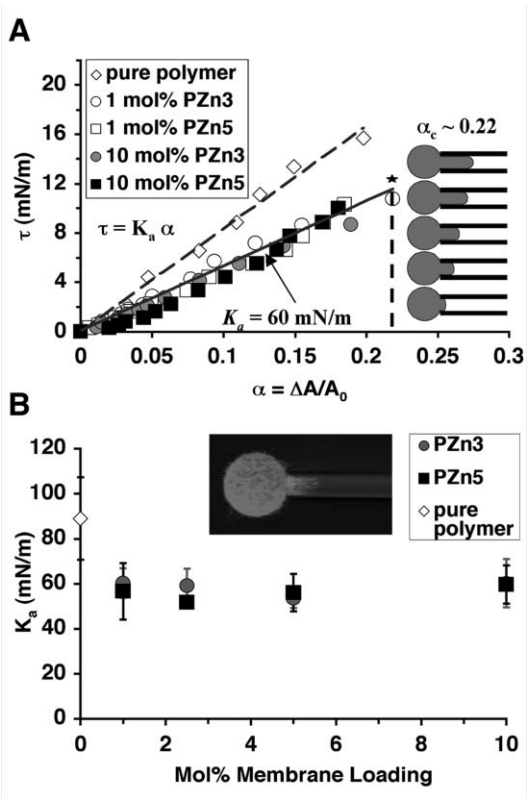

Fig. 7 Mechanical stability of PEO_{30}-b-PBD_{46}-based polymersomes loaded with oligo[porphyrin]-based fluorophores (PBFs) of various sizes. (A) Applied external tension (τ, mN m^{-1}) *vs.* areal strain (α) for unloaded vesicles and polymersomes incorporating PBFs **PZn$_3$** and **PZn$_5$**. (B) Calculated area elastic moduli (K_a, mN m^{-1}) for **PZn$_3$** and **PZn$_5$**-based polymersomes as a function of mol% membrane loading. Experimental conditions: T = 23 °C, internal aq. vesicle solution = 290 mOsm sucrose; external aq. vesicle solution = 320 mOsm PBS.

nanoscopic lamellar structure: calculated values of d and a_o where identical, within experimental error, for both loaded and unloaded vesicles. Hence, consistent with observed macromolecular effects on vesicle toughness and compliance, extensive membrane loading of hydrophobic encapsulants does not significantly disrupt intramembranous polymer chain packing nor interfere substantially with interfacial aqueous/membrane phenomena.

Experimental

Vesicle preparation

4-Hydroxybenzoate-terminated PEO_{30}-b-PBD_{46} copolymers under study were custom synthesized by Polymer Source, Inc (Dorval, Quebec Canada). **PZn$_3$** and **PZn$_5$** were synthesized following established cross-coupling methodology described elsewhere.[17] Formation of giant (>1 μm) and small (<300 nm) diameter emissive polymersomes followed procedures described in ref. 19. Briefly, 1 mM PEO_{30}-b-PBD_{46} copolymer solution and 1 mM solutions of fluorophore species in methylene chloride were combined at different molar ratios and uniformly coated on the surface of a Teflon plate, followed by evaporation of the solvent under vacuum for >12 h. The Teflon plate consisted of a 1/16″ thick sheet of Teflon cut in 1 × 1″ squares and roughened by sand paper to create macroscopically uniform digitations. Addition of aqueous solution (*e.g.* 290–310 mOsM sucrose, 290 mOsM PBS, or DI water) and heating at 60 °C for 24 h lead to

Table 1 Membrane packing characteristics in **PZn$_3$**-based polymersomes[a]

Vesicle composition (mole ratio of **PZn$_3$** : polymer)	Mol% loading	Wt% loading	d—membrane core thickness/nm	a_o—interfacial area per chain/nm^2
Pure polymer[b]	0	0	9.6[b]	1.00[b]
1 : 1000	0.1	0.08	10.40 ± 0.59	0.90 ± 0.05
1 : 100	1	0.8	10.00 ± 0.84	0.94 ± 0.08
1 : 10	10	8	10.16 ± 0.82	0.92 ± 0.07

[a] Values calculated from cryo-TEM micrographs with $n > 15$ vesicles per high power field. [b] See ref. 30.

spontaneous budding of giant (5–20 μm) emissive polymersomes (membrane loaded at prescribed polymer : fluorophore molar ratios) off the Teflon and into the aqueous surroundings. Small (<300 μm diameter) unilamellar polymersomes that possess appropriately narrow size distributions were prepared *via* procedures analogous to those used to formulate small lipid vesicles (sonication, freeze–thaw extraction, and extrusion).

Spectroscopic studies

Aqueous suspensions (in DI water) of small, unilamellar emissive polymersomes (n = 10 for each unique polymer : fluorophore formulation) were placed in 10 mm quartz optical cells and electronic absorption spectra for each of the membrane-incorporated fluorophore species were recorded on an OLIS UV/vis/NIR spectrophotometry system that is based on the optics of a Cary 14 spectrophotometer (On-line Instrument Systems Inc, Bogart, GA). The solutions were then transferred to a glass vial, frozen in liquid N_2, and lyophilized (FreeZone 4.5 L Benchtop Freeze Dry System, Labconco Corporation, Kansas City, MO; Model 77500) for 24 hours to destroy the vesicles and dry the polymer and fluorophore species. The dry samples were then taken up in the same volume of THF and their absorption spectra were recorded. The concentrations of PBF in the original polymersome solutions were calculated *via* Beer's Law using the THF absorption spectra and the previously determined average molar extinction coefficients (ε, M^{-1} cm^{-1}) for each emitter in this solvent. These calculated concentrations, as well as the original PBF absorption spectra in aqueous polymersome solutions, were then utilized in order to determine the ε for each polymersome-loaded fluorophore.

Fluorescence spectra of emissive polymersomes were obtained with a Spex Fluorolog-3 spectrophotometer (Jobin Yvon Inc, Edison, NJ) that utilizes a dual S- and T-channel configuration and PMT/InGaAs/Extended-InGaAs detectors (λ_{ex} = 510 nm). Emission spectra were corrected using the spectral output of a calibrated light source supplied by the National Bureau of Standards.

Comparison of relative fluorescence emission

Small (<300 nm diameter) vesicle suspensions (in DI water) of PEO_{30}-b-PBD_{46}- and PEO_{80}-b-PBD_{125}-based emissive polymersomes were generated by combining the respective diblock copolymers with NIRFs **PZn_3** and **PZn_5** in various molar ratios of polymer : NIRF (500 : 1, 250 : 1, 100 : 1, 40 : 1, 20 : 1, 10 : 1, 5 : 1); note, n = 3 for each unique polymer : NIRF combination. Steady-state absorption spectra for each of the solutions were recorded and 250 uL of each sample were transferred to black 96 well-plates (n = 3 plates; Becton Dickinson Co,).

Near infrared fluorescence emission from each well in the plate was then detected and quantified with an eXplore Optix Imaging System (GE Healthcare). The instrument used the following experimental parameters: 785 nm excitation laser, 785 $\pm$ 5 nm band pass excitation filter, 850 $\pm$ 50 nm band pass emission filter, 0.1 s integration time, 1 mm step size, and 25 °C stage temperature. The fluorescence emission intensity from each well in the plate was normalized by the laser power using analysis software provided by the instrument manufacturer (Analysis WorkStation 1.1.3.0, Advanced Research Technologies, Quebec, Canada). Finally, the integrated counts for each plate were divided by the NIRF concentration at the excitation wavelength (determined from the steady-state absorption spectra obtained for each emissive polymersome sample), compared, and normalized against the largest sample value.

Cryogenic transmission electron microscopy (cryo-TEM)

Specimens were prepared in a Controlled Environment Vitrification System (CEVS).[29,30] Approximately 10 μL of solution were deposited on a holey carbon film supported on a TEM grid (200 mesh, Ted Pella). Blotting the excess solution produced 100–300 nm thick films suspended in the void spaces of the holey film. Rapid immersion in liquid ethane (−181 °C) vitrified the solutions, which were then transferred to a liquid nitrogen cooled cryo-TEM holder (Gatan 626). High magnification images were obtained using a JEOL 1210 transmission electron microscope.

Micropipet aspiration

Micropipet aspiration of emissive polymersomes followed analogous procedures to those described in ref. 14. Briefly, micropipets made of borosilicate glass tubing (Friedrich and Dimmock, Milville, NJ) were prepared using a needle/pipette puller (model 730, David Kopf Instruments, Tujunga, CA) and microforged using a glass bead to give the tip a smooth and flat edge. The inner diameters of the micropipets ranged from 1 μm to 6 μm and were measured using computer imaging software. The pipettes were then used to pick up the PBF-loaded and unloaded polymersomes and apply tension to their membranes. Micropipets were filled with PBS solution and connected to an aspiration station mounted on the side of a Zeiss inverted microscope, equipped with a manometer, Validyne pressure transducer (models DP 15-32 and DP 103-14, Validyne Engineering Corp., Northridge, CA), digital pressure read-outs, micromanipulators (model WR-6, Narishige, Tokyo, Japan), and MellesGriot millimanipulators (course x,y,z control). Suction pressure was applied *via* a syringe connected to the manometer.

Experiments were performed in PBS solutions that had osmolalities of 310–320 mOsm in order to make the polymersomes flaccid (internal vesicle solution was typically 290–300 mOsm sucrose). The osmolalities of the solutions were measured using an osmometer. Since sucrose and PBS have different densities and refractive indices, the polymersomes settled in solution and were readily visible under phase-contrast or DIC optics. Near-infrared emission from the assemblies was visualized by utilizing a CCD camera, equipped with a 488 nm band-pass excitation and 650 nm long pass emission filters, and *via* fluorescence arch lamp excitation.

Conclusion

Polymersomes combine features of both natural lipid vesicles (high aqueous loading capacities) and conventional micelles

(high loading of hydrophobic compounds) in a single synthetic vesicular architecture. As such, these polymer vesicles are particularly useful for the encapsulation and delivery of a wide variety of therapeutic and imaging agents, including ones with limited to no intrinsic aqueous solubility. Here, we demonstrate that polymersome membranes can be quantitatively and reproducibly loaded at up to 10 mol/wt% concentrations through a simple method involving aqueous hydration of dry, uniform thin-films of amphiphilic polymer and the desired hydrophobic encapsulant deposited on Teflon. Polymersomes can uniquely incorporate large hydrophobic molecules that posses molecular lengths that approach up to 1/2 the core-thickness of their bilayered membranes, and which possess molecular weights comparable to those of large pharmaceutical conjugates (*e.g.* $Mw = 5.4$ kg mol^{-1}), without significantly compromising the enormous thermodynamic and mechanical stabilities of these synthetic assemblies. For biomedical applications, such large vehicle loading capacities are desirable in order to minimize the amount of associated polymer carrier, and hence maximize efficacy while curtailing any potentially new (carrier-related) toxicity. As polymersomes maintain their mechanical toughness even at high membrane-loading levels, they hold promise for the site-specific delivery of their encapsulated payloads without concomitant loss due to structural compromise in high-shear-flow vascular environments. Finally, our studies not only demonstrate the *in situ* optimization of NIR-emissive-polymersome optical properties relevant for future *in vivo* experimentation, but they also outline a basic protocol for determining loading-dependent effects of other hydrophobic molecules when incorporated within synthetic vesicle membranes. Moreover, they present a generalized paradigm for the biomimetic generation of complex multi-functional materials that combine both hydrophilic and hydrophobic agents, in a single mesoscopic structure, through cooperative self-assembly.

Abbreviations

Cryo-TEM, cryogenic transmission electron microscopy; DI, deionized; NIR, near infrared; NIRF, near infrared fluorophore; PBD, polybutadiene; PBF, multi-porphyrin-based fluorophore; PBS, phosphate buffered saline; PEO, polyethyleneoxide; PZn, [(porphinato)zinc(II)]; SOPC, 1-stearoyl-2-oleoyl-*sn*-glycero-3-phosphocholine.

Acknowledgements

This work was supported by a grant from the National Cancer Institute (RO1 CA-115229). M.J.T. and D.A.H. thank the MRSEC Program of the National Science Foundation (DMR05-20020) for infrastructural support. Cryo-TEM experiments were conducted at the MRSEC (NSF) supported Institute of Technology Characterization Facility at the University of Minnesota. D.A.H. also thanks the National Institutes of Health (EB003457-01), and P.P.G. acknowledges fellowship support from the NIH Medical Scientist Training Program and the Whitaker Foundation.

References

1 M. Shimomura and T. Sawadaishi, *Curr. Opin. Colloid Interface Sci.*, 2001, **6**, 11–16.
2 S. G. Zhang, D. M. Marini, W. Hwang and S. Santoso, *Curr. Opin. Chem. Biol.*, 2002, **6**, 865–871.
3 I. W. Hamley, *Angew. Chem., Int. Ed.*, 2003, **42**, 1692–1712.
4 O. Ikkala and G. ten Brinke, *Chem. Commun.*, 2004, 2131–2137.
5 D. D. Lasic and D. Papahadjopoulos, *Medical applications of liposomes*, Elsevier Science Ltd, Amsterdam, New York, 1998.
6 R. R. C. New, *Liposomes: A Practical Approach*, Oxford University Press, Oxford, UK, 1997.
7 V. P. Torchilin and V. Weissig, *Liposomes: a practical approach*, Oxford University Press, Oxford, New York, 2nd edn, 2003.
8 J. Cornelissen, M. Fischer, N. Sommerdijk and R. J. M. Nolte, *Science*, 1998, **280**, 1427–1430.
9 B. M. Discher, Y. Y. Won, D. S. Ege, J. C. M. Lee, F. S. Bates, D. E. Discher and D. A. Hammer, *Science*, 1999, **284**, 1143–1146.
10 D. E. Discher and A. Eisenberg, *Science*, 2002, **297**, 967–973.
11 M. Antonietti and S. Forster, *Adv. Mater.*, 2003, **15**, 1323–1333.
12 J. A. Opsteen, J. Cornelissen and J. C. M. van Hest, *Pure Appl. Chem.*, 2004, **76**, 1309–1319.
13 P. P. Ghoroghchian, G. Li, D. H. Levine, K. P. Davis, F. S. Bates, D. A. Hammer and M. J. Therien, *Macromolecules*, 2006, **39**, 1673–1675.
14 H. Bermudez, A. K. Brannan, D. A. Hammer, F. S. Bates and D. E. Discher, *Macromolecules*, 2002, **35**, 8203–8208.
15 V. S.-Y. Lin, S. G. DiMagno and M. J. Therien, *Science*, 1994, **264**, 1105–1111.
16 V. S.-Y. Lin and M. J. Therien, *Chem.–Eur. J.*, 1995, **1**, 645–651.
17 K. Susumu and M. J. Therien, *J. Am. Chem. Soc.*, 2002, **124**, 8550–8552.
18 I. V. Rubtsov, K. Susumu, G. I. Rubtsov and M. J. Therien, *J. Am. Chem. Soc.*, 2003, **125**, 2687–2696.
19 P. P. Ghoroghchian, P. R. Frail, K. Susumu, D. Blessington, A. K. Brannan, F. S. Bates, B. Chance, D. A. Hammer and M. J. Therien, *Proc. Natl. Acad. Sci. U. S. A.*, 2005, **102**, 2922–2927.
20 P. P. Ghoroghchian, P. R. Frail, K. Susumu, T. H. Park, S. P. Wu, H. T. Uyeda, D. A. Hammer and M. J. Therien, *J. Am. Chem. Soc.*, 2005, **127**, 15388–15390.
21 E. M. Sevick-Muraca, J. P. Houston and M. Gurfinkel, *Curr. Opin. Chem. Biol.*, 2002, **6**, 642–650.
22 R. Weissleder and V. Ntziachristos, *Nat. Med.*, 2003, **9**, 123–128.
23 F. Ricchelli, *J. Photochem. Photobiol., B*, 1995, **29**, 109–118.
24 V. V. Borovkov, M. Anikin, K. Wasa and Y. Sakata, *Photochem. Photobiol.*, 1996, **63**, 477–482.
25 K. Lang, J. Mosinger and D. M. Wagnerova, *Coord. Chem. Rev.*, 2004, **248**, 321–350.
26 A. Gilbert and J. E. Baggott, *Essentials of Molecular Photochemistry*, Blackwell Science, Oxford, UK, 1991.
27 E. Evans and A. Yeung, *Chem. Phys. Lipids*, 1994, **73**, 39–56.
28 E. Evans and D. Needham, *J. Phys. Chem.*, 1987, **91**, 4219–4228.
29 J. R. Bellare, H. T. Davis, L. E. Scriven and Y. Talmon, *J. Electron Microsc.*, 1988, **10**, 87–111.
30 Y. Y. Won, A. K. Brannan, H. T. Davis and F. S. Bates, *J. Phys. Chem. B*, 2002, **106**, 3354–3364.

